Influence of imperfect joints and geometrical tolerances on a circuit breaker dynamics

Narendra Akhadkar[1], Vincent Acary[2], and Bernard Brogliato[2]

[1]Schneider Electric, 2 Chemin des sources, 38240, Meylan, France,
narendra.akhadkar@se.com
[2]Univ. Grenoble-Alpes, INRIA, CNRS, Grenoble INP, LJK, 38000 Grenoble, France,
vincent.acary@inria.fr, bernard.brogliato@inria.fr

Abstract. The aim of this paper is to understand the in uence of clearances in the kinematic joints, dimensional and geometrical tolerances associated with the parts, on the performance of a circuit breaker mechanism in the trip operation. Operating mechanism and trip unit are the essential components of a miniature circuit breaker. The operating and trip mechanisms are made of ten parts with revolute and cylindrical joints with clearance, and ve unilateral contacts with friction. This mechanism is based on quick-make and quick-break principle. The Moreau-Jean nonsmooth contact dynamics (NSCD) numerical method is used to perform the simulations. The numerical results are validated by careful comparisons with experimental data.

Keywords: Joint clearance; geometrical tolerances; unilateral constraints; Coulomb s friction; impacts; circuit breaker.

1 Introduction

The important function of a circuit breaker is to switch ON/OFF/TRIP the electrical current, and to protect the lowest common distributed voltage in an electrical system. It plays a vital role to safeguard the electrical system in the event of electrical short circuit and overload conditions. Trip unit activates the electromagnetic tripping mechanism to break the current ow in the electrical system/network. The time duration to break the current ow is few milliseconds, and any delay in tripping function can create hazardous conditions, where human safety can not be guaranteed. Usually, the performance of circuit breaker mechanisms is not as desired, due to various factors such as manufacturing dimensional and geometrical tolerances on the parts, clearances in the joints and the assembly tolerances. These factors are directly linked to the manufacturing cost of the product, and it is important to optimize the product cost and to guarantee the desired overall performance of the product. In the computer models, it is always assumed that the geometry of the real part is perfect. In reality the surfaces are subject to irregularities such as bumps, undulations and surface roughness [1]. Geometric tolerances are always de ned by the tolerance band with upper and lower limit of acceptance. It is assumed that the real surface must lie inside this tolerance band [1, 12, 16].

Clearance in the spatial revolute (resp. cylindrical) joint adds ve (resp. four) extra degrees of freedom into the system. Most of the previous work is focused on

T. Uhl (ed.), *Advances in Mechanism and Machine Science*,
Mechanisms and Machine Science 73,
https://doi.org/10.1007/978-3-030-20131-9_302

the radial clearance in the planar and spatial revolute and cylindrical joints [14, 18, 17]. However, more recently the in uence of the axial clearance in the revolute joint has been studied in [22, 23].

Most of the mechanisms in the Schneider Electric company use frictional contacts and the compliant models cannot correctly model the sticking condition. The nonsmooth modeling approach together with an event-capturing time-stepping scheme allows us to simulate, in an ef cient and robust way, the contact and impacts phenomena that occur in joints with clearances. In the nonsmooth contact dynamic (NSCD) approach, the interaction of the colliding bodies is modeled with multiple frictional unilateral constraints [19, 20]. The unilateral constraints are described by set-valued force laws in normal and tangential directions. The normal contact law is based on Signorini s condition while the tangential contact law is based on Coulomb s friction law. Careful comparisons between numerical results obtained with the NSCD approach, and experimental data are reported in [21, 24], while the use of the NSCD approach for systems with clearances is also advocated in [15, 8, 10]. They demonstrate that the numerical schemes and the model used in this article, though they can be improved, possess very good forecast capabilities.

Our aim is to study the in uence of clearance in the kinematic joints, dimensional and geometrical tolerances on the tripping function of the miniature circuit breaker, in the three dimensional case. This article is an extension of the work presented in [9]. Another objective is to develop a virtual test bench using the INRIA open-source simulation software SICONOS[1]. Our aim is to validate the simulation model, experiments are carried-out on the prototype samples and the results are compared with the simulations.

The article is organized as follows: in Section 2, the kinematics and dynamics are presented. Section 3, is dedicated to the detailed description of the circuit breaker mechanism and modeling of geometrical tolerances. In Section 4, numerical results are compared with experimental data and conclusions are in Section 5.

2 Formulation of the nonsmooth dynamical systems

2.1 Normal and tangential contact laws

Let us consider two non overlapping bodies (see Fig. 1), a potential contact point between two bodies is given by the closest points C_A and C_B. A local frame is de ned at the potential contact point by $(\mathsf{N}, \mathsf{T}_1, \mathsf{T}_2)$. The gap g_{N} is de ned as the signed distance between the two potential contacting points C_A and C_B. The contact force is denoted as $r = (r_{\mathrm{N}}, r_{\mathrm{T}})^{\top} \in I\!R^3$. Due to the impenetrability assumption, one has $g_{\mathrm{N}} \geqslant 0$. We also neglect adhesive effects so that $r_{\mathrm{N}} \geqslant 0$. If $r_{\mathrm{N}} > 0$ then we impose $g_{\mathrm{N}} = 0$, and when $g_{\mathrm{N}} > 0$, the normal contact force must vanish, *i.e.* $r_{\mathrm{N}} = 0$ (no magnetic or distance forces) [4, 6, 11]. These conditions yield a complementarity condition denoted compactly as:

$$0 \leqslant g_{\mathrm{N}} \perp r_{\mathrm{N}} \geqslant 0. \tag{1}$$

The normal contact law at the velocity level is expressed as :

$$0 \leqslant u_{\mathrm{N}} \perp r_{\mathrm{N}} \geqslant 0, \quad \text{if } g_{\mathrm{N}} = 0. \tag{2}$$

[1] http://siconos.gforge.inria.fr/

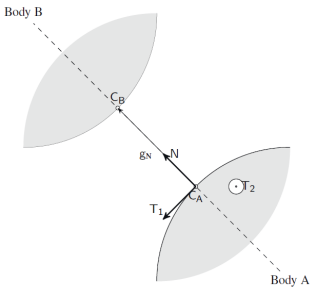

Fig. 1: Contact local frame.

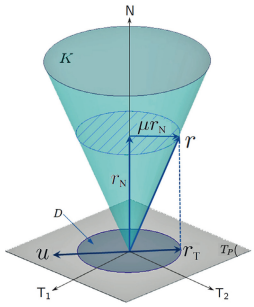

Fig. 2: 3D Coulomb's friction cone, sliding case.

The tangential contact law is the Coulomb friction that constrain the contact force r in the the friction cone (see Fig. 2)

$$r \in K = \{r \in I\!R^3, ||r_T|| \leqslant \mu r_N\}. \tag{3}$$

The scalar $\mu \geqslant 0$ is the coefficient of friction. In case of sliding, the tangential force r_T acts in direction opposite to the relative tangential velocity u_T. If the relative tangential velocity u_T is zero, then the bodies stick to each other (rolling without slipping). We introduce the modified relative velocity $\widehat{u} := u + \mu \|u_T\| \mathsf{N}$, then the Coulomb friction can be equivalently expressed as a second–order cone complementarity condition [13, 7] if $g_N = 0$:

$$K^* \ni \widehat{u} \perp r \in K. \tag{4}$$

The cone $K^* = \{v \in I\!R^3 | r^T v \geqslant 0,\ \forall r \in K\}$ is the dual cone of K.

2.2 Newton-Euler formulation of the equation of motion

Let us consider a mechanical system subjected to m constraints, with m_e holonomic bilateral constraints $h^\alpha(q) = 0, \alpha \in \mathscr{E} \subset I\!N$, m_i unilateral constraints $g_N^\alpha(q) \geqslant 0, \alpha \in \mathscr{I} \subset I\!N$ and Coulomb friction. The Newton-Euler formulation of such a system is given as:

$$\left\{\begin{array}{lll}
\dot{q} = T(q)v, & & \\
M\dot{v} = F(t,q,v) + H^\top(q)\lambda + G^\top(q)r, & & \\
H^\alpha(q)v = 0, & & \alpha \in \mathscr{E} \\
\left.\begin{array}{lll}
u^\alpha = G^\alpha(q)v, & \widehat{u}^\alpha = u^\alpha + \mu^\alpha \|u_T^\alpha\| \mathsf{N}^\alpha & \\
r^\alpha = 0, & \text{if } g_N^\alpha(q) > 0, & \\
K^{\alpha,*} \ni \widehat{u}^\alpha \perp r^\alpha \in K^\alpha, & \text{if } g_N^\alpha(q) = 0, & \\
u_N^{\alpha,+} = -e_r^\alpha u_N^{\alpha,-}, & \text{if } g_N^\alpha(q) = 0 \text{ and } u_N^{\alpha,-} \leqslant 0, &
\end{array}\right\} & & \alpha \in \mathscr{I}
\end{array}\right.$$

where q is the vector of coordinates of the position and the orientation of the body, v is the velocity, the operator $T(q) \in I\!R^{7\times 6}$ links the time derivatives of the coordinates to the velocities, M is the total inertia matrix, $F(t,q,v) \in I\!R^6$

collects all the forces and torques applied to the body. The operators $H \in \mathbb{R}^{m_e \times n}$ and $G \in \mathbb{R}^{3m_i \times n}$ link the local velocity variables in the joints, and at contacts respectively, to the velocity vector of the bodies.

2.3 The numerical integration method

In this paper we use the event–capturing method based on the Moreau–Jean time-stepping scheme [6, 19, 20], where the constraints are solved at the velocity level, and thereafter named the NSCD method. It is well–known that velocity level treatment of constraints yields violations of constraints with the drift phenomenon. When we simulate mechanisms with small clearances, this is not tolerable, since we have to keep the violation as small as possible with respect to the characteristic length of the clearances. To overcome this limitation of the standard Moreau–Jean time-stepping scheme, we use the combined projection scheme as proposed in [5].

3 The C-60 miniature circuit breaker mechanism

A miniature circuit breaker consists of operating mechanism, trip unit, arc chute, electrical contacts enclosed in insulated housing. Important functions of a circuit breaker are: to **s**ense the over-current in the electrical network, **m**easure the amount of over-current owing, and to **a**ct by tripping the operating mechanism to break the contacts in a timely manner to ensure human safety and to prevent damage. A typical miniature circuit breaker mechanism with trip unit is depicted

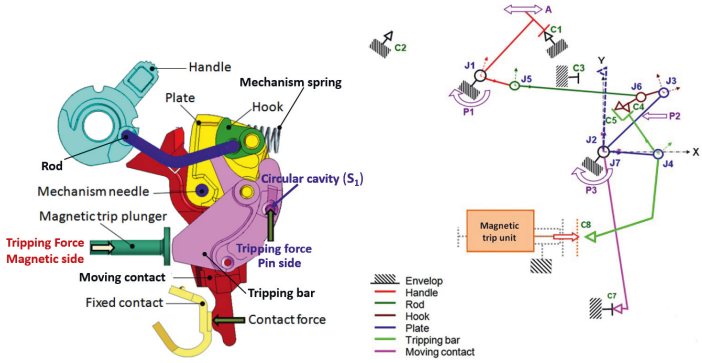

(a) Front view. (b) Kinematic representation.

Fig. 3: C-60 circuit breaker mechanism - ON position.

in Fig. 3(a).

Mechanism working principle: All the mechanism parts are enclosed in-between the case and cover parts. These parts are connected to each other through a kinematic joint or frictional contact. In the following section we will see the detailed

description of these kinematic joints and contacts. In the first step, the primary function of a mechanism is usually formulated in terms of kinematical quantities (link geometry, kinematic constraints, *etc*). Also the various geometrical relations resulting from the kinematical analysis of the linkage mechanism are an essential ingredient for the dynamic analysis. The kinematical analysis of a miniature circuit breaker mechanism (hereafter called the C-60 mechanism) is of great importance. The C-60 operating mechanism consists of seven links, seven revolute joints with clearance in both radial and axial direction and four frictional contacts (see Fig. 3(b)). It has 42 degrees of freedom. The trip unit through trip mechanism determines when the contacts will open automatically. A trip mechanism is held in place by the tripper bar (see Fig. 3(a)). As long as the tripping bar holds the trip mechanism, the mechanism remains firmly locked in place and remains in ON position.

The operating mechanism in the ON and TRIP position is explained as follows:

The close operation leads to ON position of the breaker. The operating handle (A) is rotated clockwise which closes the contacts C_5 and C_4 through the revolute joints J_1, J_5, J_6, J_3 and J_4. The frictional contacts C_5 and C_4 have a specific wedge shape profile, which enables the locking between the hook and tripping bar. After the activation of the contacts C_5 and C_4 the motion has been transferred to the moving contact through the plate by revolute joints J_2 and J_7, which ensure closing of the contact between the moving and the fixed contact. During close operation the handle spring (P_1) and the mechanism springs (P_2 and P_3) get charged, which will be used for the trip operation of the breaker.

The Trip operation leads to TRIP position of the breaker. In the trip operation (see Figure 3(b)), the activation of the tripping coil causes the tripping plunger of the trip mechanism to be attracted, thus releasing the contact C_7 through C_3 and C_4. In response, the handle and mechanism springs discharge by moving the handle and plate to the open position.

3.1 Geometrical tolerances

Geometrical tolerances are divided into three categories: form, orientation and position tolerances. In this study we focused mainly on the position and orientation tolerances [1–3] and their influence on the C-60 breakers performance. The position tolerance can be divided in two types such as, simple and bidirectional position. In case of the simple position tolerance, the zone of tolerance is bounded by two parallel planes at a distance t, and placed symmetrically with respect to the theoretically exact position of the surface under consideration. In the bidirectional position tolerance, the value of tolerance is defined by the zone of tolerance which is bounded by a cylinder of diameter t, whose axis is in the theoretically exact position of the line under consideration, if the value of tolerance is preceded by the symbol $\varnothing$ (see Figure 4).

3.2 Modeling of the geometrical tolerances in SICONOS

The position tolerance is modeled by varying the position of the bearing axis from the reference axis (datum) (see Figure 5). We have considered the two extreme cases, *i.e.*, LSL and USL of the position tolerance on the axis of bearing. With these two axis positions, we can create the 3D CAD model of the bearing. In Fig-

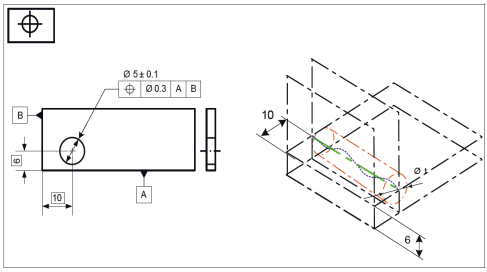

Fig. 4: Position tolerance-Axis position.

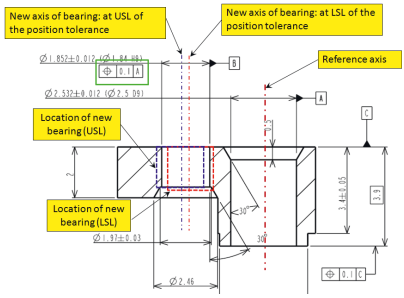

Fig. 5: Modeling of the position geometrical tolerances in SICONOS.

ure 5, the new locations of the bearing are shown with blue and red colors dotted lines along with the new bearing axis. In this way we can simulate two different cases of the geometrical tolerances. The CAD model is developed for this case and used for the simulations. The major conclusions are: **(i)** In case of the dimensional and geometrical variation combined together, approximately the maximum variation of 10% is observed on the geometrical position of Y-coordinate of the circular cavity (S_1) center from the mechanism needle axis when compared to the case dimensional tolerance (see Table 1). **(ii)** In case of the contact and tripping force, the total variation more than 15% is observed between the case of dimensional and dimensional with geometrical (combined) tolerance (see Table 1). **(iii)** The variations in the functional conditions due to geometrical tolerances may increase if all the geometrical variations (position, orientation and form tolerances) are considered together. However, the process of modeling all these variations in the CAD model is quite tedious task.

4 Experimental validation: Pin side tripping force versus displacement

In this section we report comparisons between numerical results obtained with the NSCD method, and experimental data obtained on physical prototypes built by Schneider Electric. There are two different ways a C-60 breaker can be tripped: **(i)** pin side tripping and **(ii)** magnetic side tripping, see Fig. 3(a). In the pin

Table 1: Comparison between the in uence of radial clearance and geometrical tolerance.

Functional condition	Equal radial clearance in all the joints (mm)			% relative error $e_{c/g} = \frac{A^{ref} - A^{c/g}}{A^{c/g}} \times 100$	
	0.01 mm A^{ref}	0.05 mm A^{c}	0.05 mm + Geometrical tolerance (A^{g})	e_c	e_g
Contact Force	7.526	6.935	6.581	-7.85	-15.56
X-coordinate center of S_1	10.749	10.710	10.501	-0.37	-2.30
Y-coordinate center of S_1	4.534	4.269	4.102	-5.84	-9.54
Pin side Tripping Force	2.015	1.873	1.752	-7.58	-15.01

side tripping, circular cavity S_1 on the tripping bar is used for the application of external force to trip the C-60 breaker. For the magnetic side tripping, magnetic trip plunger is used for the application of external force to trip the C-60 breaker(see Fig. 3(a)) The tripping operation is possible only if the product is in ON condition. In the case of pin-side tripping, the The radial clearance in the revolute joints is given as: $J_1 = 0.085$mm, $J_2 = 0.05$mm, $J_3/J_4 = 0.06$mm, $J_5/J_6 = 0.045$mm and $J_7 = 0.055$mm. Referring to the tripping force (pin side) arrow in Fig. 3(a), the comparisons are made by recording force and displacement histories at the center of circular cavity S_1 on the tripping bar. The test bench consists of the

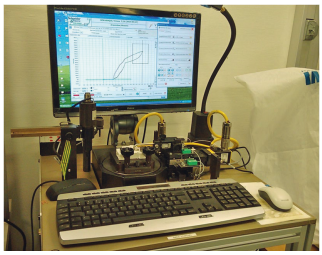

Fig. 6: Experimental test bench for tripping force measurement.

xture to mount the C-60 breaker and the moving table which comprises a pair of linear motion guide, see Fig. 6. The load cell is mounted on the moving table to measure the force and the bi-axial movement of the moving table is measured by two position sensors. The tripping operation is possible only if the product is in ON condition. The major conclusions are: **(i)** In case of the experimental results, the recorded peak force is 1.77 N at a distance of 0.27 mm. The total trip distance is 0.44 mm (see Figure 7(a)). In case of the virtual test, the trajectory of the trip-

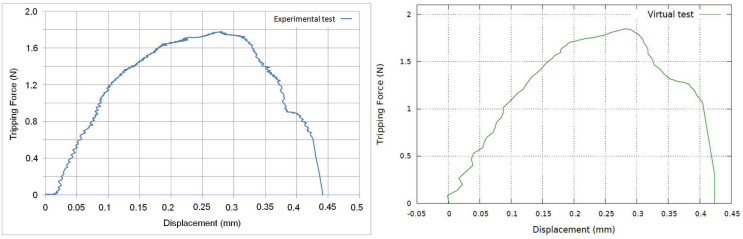

(a) Experimental test (b) Virtual test

Fig. 7: Pin side - Tripping force vs Displacement.

ping force is slightly different when compared to the experimental results (see Figure 7(b)). The total trip distance is 0.42 mm, and the variation of 0.02 mm is seen between the virtual and experimental test results. However the peak force in case of virtual test is 1.87 N and when compared to the experimental results the variation is 0.1 N (see Figure 7(a)-(b)). **(ii)** It is evident from the trajectory of the tripping force that only the front-side contacts are made. However the location of the contact points may vary from assembly to assembly. After careful study of the tripping force trajectory on the mass production samples, it is observed that the number of contacts may vary from sample to sample and the tripping force is also varying. The results between the experimental and virtual model shows good match (see Figure 7(a)-(b)).

4.1 Virtual test: influence of joint clearances and geometrical tolerances on magnetic side tripping operation

The virtual test models are built with radial clearance in all the kinematic joints and geometrical tolerances on the parts. The position of the tripping bar in ON condition is set as the reference position. Distance between the magnetic trip plunger and tripping bar in ON condition is set as the reference position, see Figure 3(a). External force is applied at the left side of the tripping bar with the help of magnetic trip unit through magnetic trip plunger, see Figure 3(a)-(b). The simulations are carried out with different values of joint clearances and geometrical tolerances and the results are plotted, see Figure 8. We have considered equal radial clearance in all the revolute joints J_1 to J_7 . The important conclusions are: **(i)** In case of magnetic-side tripping, as the radial clearance in the revolute joint and geometrical tolerance increases, then the tripping force decreases and the tripping distance increases. **(ii)** The increase in the tripping distance is responsible for delay in the tripping operation and could lead to catastrophic failure. **(iii)** Reduction in the tripping force could lead to nuisance tripping which will result in undesired power failure.

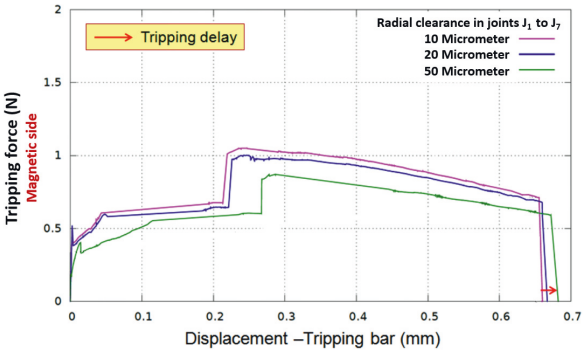

Fig. 8: Magnetic side - Tripping force vs Displacement.

5 Conclusions

This paper is devoted to the numerical simulation of the C-60 circuit breaker built by Schneider Electric, using the so-called Moreau-Jean NSCD event-capturing numerical scheme. It relies on rigid body assumptions, with set-valued Coulomb s friction, and constant kinematic restitution coef cients. Emphasis is put on the modeling of three dimensional kinematic joints with clearance and geometrical tolerance. It is found that the geometrical tolerances plays a signi cant role in the tripping operation of a circuit breaker. Moreover detailed comparisons with experimental date obtained at the Schneider Electric laboratory, prove the very good prediction capabilities of the NSCD approach, for this kind of mechanisms.

References

1. ISO-1101: Geometrical Product Speci cations (GPS) – Geometrical tolerancing – Tolerances of form, orientation, location and run-out. International Organization for Standardization (2012)
2. ISO-5458: Geometrical Product Speci cations (GPS) – Geometrical tolerancing – Positional tolerancing. International Organization for Standardization (2018)
3. ISO-5459: Geometrical Product Speci cations (GPS) – Geometrical tolerancing – Datums and datum systems. International Organization for Standardization (2018)
4. Abadie, M.: Dynamic simulation of rigid bodies: Modelling of frictional contact. In: B. Brogliato (ed.) Impacts in Mechanical Systems: Analysis and Modelling, *Lecture Notes in Physics (LNP)*, vol. 551, pp. 61–144. Springer (2000)
5. Acary, V.: Projected event-capturing time-stepping schemes for nonsmooth mechanical systems with unilateral contact and Coulomb s friction. Computer Methods in Applied Mechanics and Engineering **256**, 224–250 (2013)
6. Acary, V., Brogliato, B.: Numerical Methods for Nonsmooth Dynamical Systems. Applications in Mechanics and Electronics. Lecture Notes in Applied and Computational Mechanics 35. Berlin: Springer. xxi, 525 p. (2008)

7. Acary, V., Cadoux, F., Lemarechal, C., Malick, J.: A formulation of the linear discrete Coulomb friction problem via convex optimization. ZAMM-Journal of Applied Mathematics and Mechanics/Zeitschrift für Angewandte Mathematik und Mechanik **91**(2), 155–175 (2011)
8. Akhadkar, N., Acary, V., Brogliato, B.: Analysis of collocated feedback controllers for four-bar planar mechanisms with joint clearances. Multibody System Dynamics **38**(2), 101–136 (2016)
9. Akhadkar, N., Acary, V., Brogliato, B.: 3D revolute joint with clearance in multibody systems. In: Computational Kinematics, pp. 11–18. Springer (2018)
10. Akhadkar, N., Acary, V., Brogliato, B.: Multibody systems with 3D revolute joints with clearances: an industrial case study with an experimental validation. Multibody System Dynamics **42**(3), 249–282 (2018)
11. Brogliato, B.: Nonsmooth Mechanics: Models, Dynamics and Control, 3rd edn. Springer-Verlag, London (2016)
12. Colosimo, B., Senin, N.: Geometric Tolerances. Springer (2010)
13. De Saxcé, G.: Une généralisation de l inégalité de Fenchel et ses applications aux lois constitutives. C.R.A.S. Paris **t 314,série II**, 125–129 (1992)
14. Flores, P.: A parametric study on the dynamic response of planar multibody systems with multiple clearance joints. Nonlinear Dynamics **61**(4), 633–653 (2010)
15. Flores, P., R.Leine, Glocker, C.: Modeling and analysis of planar rigid multibody systems with translational clearance joints based on the non-smooth dynamics approach. Multibody System Dynamics **23**, 165–190 (2010)
16. Gauthier, L.: General principles and rules for technical drawing. Technical Note FT15 057
17. Gummer, A., Sauer, B.: In uence of contact geometry on local friction energy and stiffness of revolute joints. Journal of tribology **134**(2), 021,402 (2012)
18. Haroun, A., Megahed, S.: Simulation and experimentation of multibody mechanical systems with clearance revolute joints. In: Proceedings of World Academy of Science, Engineering and Technology, 63. World Academy of Science, Engineering and Technology (2012)
19. Jean, M.: The non-smooth contact dynamics method. Computer Methods in Applied Mechanics and Engineering **177**(3), 235–257 (1999)
20. Jean, M., Moreau, J.: Dynamics in the presence of unilateral contacts and dry friction: a numerical approach. In: G. del Piero, F. Maceri (eds.) Unilateral Problems in Structural Analysis II, no. 304 in CISM Courses and Lectures, pp. 151–196. Springer Verlag (1987)
21. Krinner, A., Thümmel, T.: Non-smooth behaviour of a linkage mechanism with revolute clearance joints. In: New Advances in Mechanisms, Transmissions and Applications, pp. 233–241. Springer (2014)
22. Orden, J.G.: Analysis of joint clearances in multibody systems. Multibody System Dynamics **13**(4), 401–420 (2005)
23. S.Yan, Xiang, W., Zhang, L.: A comprehensive model for 3d revolute joints with clearances in mechanical systems. Nonlinear Dynamics pp. 1–20 (2014)
24. T. Thümmel and K. Funk: Multibody modelling of linkage mechanisms including friction, clearance and impact. In: Proceedings of the 10th World Congress on the Theory of Machines and Mechanisms in Oulu, June 20 to 24, vol. 4, pp. 1387–1392. Oulu University Press, Finland (1999)